

## BRIEF COMMUNICATIONS

The purpose of this Brief Communications section is to present important research results of more limited scope than regular articles appearing in *Physics of Fluids*. Submission of material of a peripheral or cursory nature is strongly discouraged. Brief Communications cannot exceed three printed pages in length, including space allowed for title, figures, tables, references, and an abstract limited to about 100 words.

### The wall-normal position in pipe and channel flows at which viscous and turbulent shear stresses are equal

Anupam Sahay and Katepalli R. Sreenivasan

Mason Laboratory, Yale University, New Haven, Connecticut 06520-8286

(Received 26 May 1999; accepted 23 June 1999)

The Reynolds number dependence is estimated for the wall-normal position at which the turbulent and viscous shear stresses are equal. For large Reynolds numbers, this position coincides with the peak location of the mean momentum transport terms due to turbulent and viscous action. Experimental data are used to corroborate the results and assess some quantitative details. © 1999 American Institute of Physics. [S1070-6631(99)02410-1]

In wall-bounded turbulent flows, it is believed that the statistics of turbulence very close to the wall scale on wall variables alone, independent of the bulk Reynolds number of the flow. The wall variables are the friction velocity  $U_*$  ( $\equiv \sqrt{\tau_w/\rho}$ , where  $\tau_w$  is the wall shear stress and  $\rho$  is the fluid density) and the kinematic viscosity  $\nu$ . Empirical evidence<sup>1,2</sup> suggests that this is indeed true as a first approximation. However, a closer inspection of the data<sup>3</sup> reveals that even quantities measured very near the wall show some Reynolds number dependence. It is important to understand such dependencies because they offer clues to the inner-outer interaction, which is the key feature of wall-flows.<sup>4</sup> We examine here the Reynolds number dependence of the wall-normal position at which the turbulent shear stress equals the viscous stress, and relate it to those positions at which turbulence production and momentum transport attain their respective maxima. We shall restrict attention to fully developed channel and pipe flows.

All the quantities to be used here are normalized by wall variables, so we dispense with the conventional notation of using the suffix “+” to identify them. The wall-normal coordinate is  $y$ . The mean momentum equation is then exactly

$$\tau_t(y, R_*) + \tau_v(y, R_*) = 1 - y/R_*, \quad (1)$$

where  $\tau_t$  and  $\tau_v$  are the turbulent and viscous shear stresses and  $R_* \equiv U_* h/\nu$ ,  $h$  being the channel half-height or pipe radius. If we denote the position where  $\tau_t = \tau_v$  as  $\tilde{y}$  and the common stress value there as  $\tilde{\tau}$ , then we have from (1)

$$\tilde{\tau} = \frac{1}{2}(1 - \tilde{y}/R_*). \quad (2)$$

The limiting value of  $\tilde{\tau}$  is, of course,  $\frac{1}{2}$ . Let  $\tilde{y}_\infty = \lim_{R_* \rightarrow \infty} \tilde{y}$ . The boundedness of  $\tilde{y}$  follows from the em-

pirical fact that in channel and pipe flows the viscous stress decreases monotonically with  $y$  and has significant support only in a thin layer adjacent to the wall. It then follows that

$$\tilde{y} = \tilde{y}_\infty + f(R_*), \quad (3)$$

where  $f(R_*)$  is an unknown function of  $R_*$  with  $\lim_{R_* \rightarrow \infty} f(R_*) = 0$ .

Before discussing the nature of  $f(R_*)$ , we may relate  $\tilde{y}$  to the position of the peak turbulence production location,  $y_p$ . The product of the turbulent and viscous stresses ( $P = \tau_t \tau_v$ ) is the production of turbulent energy by way of its extraction from the mean flow. On differentiating  $P$  with respect to  $y$  (the derivatives being denoted by the overset dot) and using Eq. (1), we have, at the position of peak production,

$$\frac{\tau_t}{\tau_v} = - \frac{\dot{\tau}_t}{\dot{\tau}_v} = 1 + \frac{1}{R_* \dot{\tau}_v}. \quad (4)$$

Because the viscous stress decays monotonically with the distance from the wall,  $\dot{\tau}_v$  is negative definite, and it follows from Eq. (4) that  $\tau_t \leq \tau_v$  at  $y_p$ . In turn, this implies, again because of the monotonic decay of  $\tau_v$ , that  $y_p \leq \tilde{y}$ . That is, the peak of the production occurs no further from the wall than the point where the turbulent and viscous stresses are equal. In the limit  $R_* \rightarrow \infty$ ,  $y_p$  will trivially coincide with  $\tilde{y}$  [from the property of the function  $x(1-x)$ ].

Let us now consider the positions of extrema of the two transport terms,  $\dot{\tau}_t$  and  $\dot{\tau}_v$ . Their sum is constant in  $y$ , equal to the mean pressure gradient driving the flow. This follows from differentiating (1) with respect to  $y$ . The constancy of the sum of the transport terms implies that their extrema will

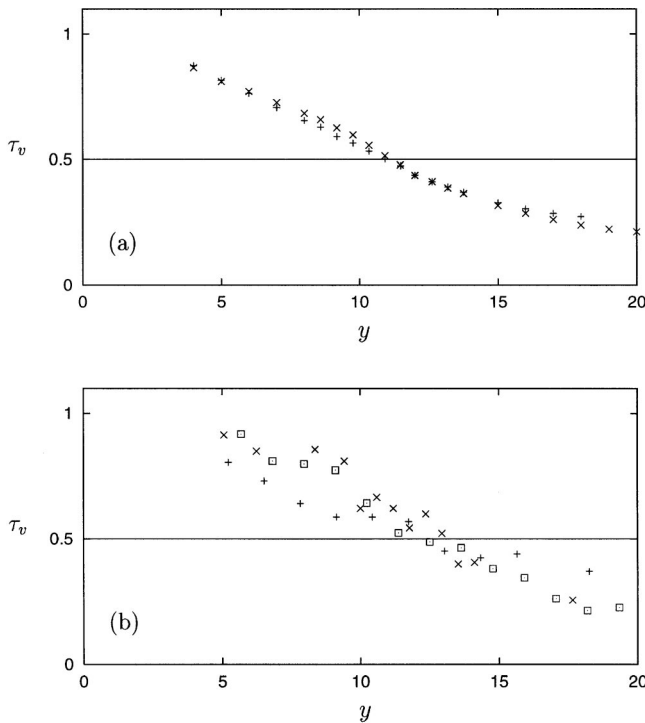


FIG. 1. Viscous stress  $\tau_v$  near the wall in turbulent channel flows. The data in (a), from Eckelmann (Ref. 5) for  $[+]$   $R_* = 142$  and  $[ \times ]$   $R_* = 208$ , were obtained directly from the published plot of the turbulent shear stress  $\tau_v$ . The data in (b), from Laufer (Ref. 6) for  $[+]$   $R_* = 522$ ,  $[ \times ]$   $R_* = 1177$ , and  $[ \square ]$   $R_* = 2275$ , were obtained by differentiating (using center difference) the mean velocity data.

coincide, say at  $y_m$ . The limiting behavior of  $y_p$  in conjunction with Eq. (4) implies that  $y_m$  will coincide with  $y_p$  for large  $R_*$ .

We now turn to experimental data to assess the numerical value of  $\tilde{y}_\infty$  and the functional form of  $f(R_*)$ . First, we should note that accurate measurements near the wall are hard to make, and so a consistency check would be desirable. Experimentally, the quantities  $\tilde{y}$  and  $\tilde{\tau}$  are independently measured quantities, and so can be checked against Eq. (2). The outcome of this test is quite satisfactory.

The sign of  $f(R_*)$  can be discerned as follows. Figures 1(a) and 1(b) show, for two different sets of experiments,  $\tau_v$  as a function of  $y$  near the wall in turbulent channel flows. The shape of  $\tau_v$  does not seem to change with  $R_*$  for the low Reynolds number data [Fig. 1(a)], but shows a modest shift towards the wall in the high Reynolds number data [Fig. 1(b)]. A conservative statement is that the position of  $\tau_v = 0.5$  does not move away from the wall as  $R_* \rightarrow \infty$ . This fact, in conjunction with the monotonic decay of  $\tau_v$ , implies that  $f(R_*) \geq 0$ . That is, the  $\tilde{y}$  approaches  $y_\infty$  from above.

To determine the shape of  $f(R_*)$ , we use experiments in conjunction with Eq. (3) and Eq. (1), the latter rewritten as

$$1 - 2\tilde{\tau} \sim \frac{\tilde{y}_\infty}{R_*} + \frac{f(R_*)}{R_*} \quad (R_* \rightarrow \infty). \quad (5)$$

The function  $f$  could decay with  $R_*$  like  $R_*^{-\alpha}$ , where  $\alpha > 0$ , or like  $1/\ln R_*$ , or take a more complex form. It is prudent to consider the two simplest situations just men-

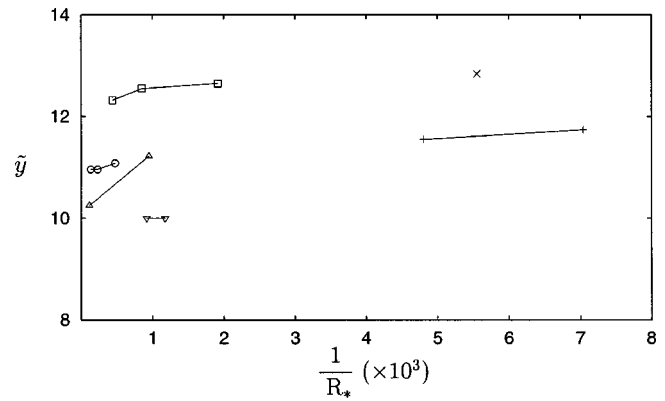


FIG. 2. Variation of  $\tilde{y}$  with Reynolds number  $R_*$ . Data from the same source are joined by a line. Experimental data:  $[+]$  Eckelmann (Ref. 5) (Channel,  $R_* = 142, 208$ );  $[ \square ]$  Laufer (Ref. 6) (Channel,  $R_* = 522, 1177, 2275$ );  $[ \times ]$  Kim *et al.* (Ref. 7) (Channel, DNS,  $R_* = 180$ );  $[ \circ ]$  Comte-Bellot (Ref. 8) (Channel,  $R_* = 2117, 4324, 7309$ );  $[ \triangle ]$  Laufer (Ref. 1) (Pipe,  $R_* = 1055, 8250$ );  $[ \nabla ]$  Zagarola (Ref. 9) (Channel,  $R_* = 850, 1090$ ). Although the scatter from different sources mask possible Reynolds number trend, each set of data shows a decreasing trend with increasing Reynolds number.

tioned; upon testing them both, we lean towards the power-law behavior—this being consistent with the tradition in the asymptotic analyses of turbulent flows.

Figure 2 shows a plot of  $\tilde{y}$  with  $1/R_*$  for various channel and pipe flows. Clearly, no universal curve of the form (3) can be fitted to all the data, and systematic errors may in fact account for the observed differences among the various experiments. One also has to allow for the possibility that  $\tilde{y}_\infty$  is different for pipes and channel flows. In spite of these uncertainties, one trend that seems to stand out in the plot is that, within a given set of experiments (represented by the same symbols and joined by lines for clarity),  $\tilde{y}$  does decrease with increasing  $R_*$ . This is consistent with  $f$  being nonnegative definite. The scatter in the data does not allow us to specify  $\tilde{y}_\infty$  to better accuracy than between 10 to 12; we pick the average value of 11 (and make no distinction between channel and pipe flows).

By subtracting  $\tilde{y}_\infty/R_*$  from  $1 - 2\tilde{\tau}$ , we should have the functional form of  $f(R_*)/R_*$ . This quantity is plotted in Fig. 3 against  $1/R_*$ . Motivated by the prejudice for power laws, we have attempted various fits of the form  $f(R_*) = a/R_*^m - b/R_*^{2m}$  to the data. The one with the least error

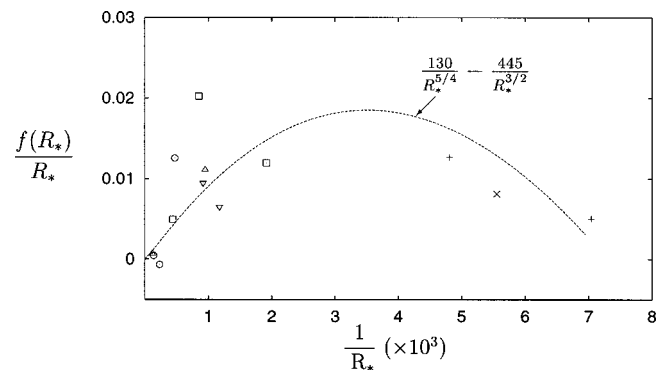


FIG. 3. Variation of  $f(R_*)/R_*$  with  $1/R_*$ , as described in the text. The symbol key is the same as in Fig. 2.

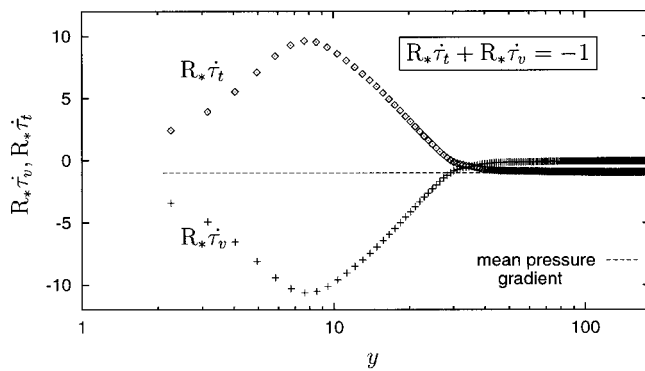


FIG. 4. Mean momentum transport normalized by the mean pressure gradient. Calculation of the transport terms involved differentiating the mean velocity data twice. Thus, the location of the peaks and the magnitudes of the transport terms may be uncertain. The figure shows unmistakably that the balance near the wall involves the difference between two large terms. The data are from Kim *et al.* (Ref. 7) at  $R_* = 180$ .

corresponds to  $m = \frac{1}{4}$ . This fit, shown in Fig. 3, appears to be an adequate representation of the data. Note that this non-monotonic behavior of  $f(R_*)$  arises because we have considered both low and high Reynolds number data; consideration of only the high Reynolds number data yields just the first term (or a slight modification of it).

Another useful observation, ensuing from the limit of  $y_p$  and from (4), relates to the ratio of the magnitude of the viscous transport term to the mean pressure gradient ( $R_* \dot{\tau}_v$ ). This ratio will increase without bounds as  $R_* \rightarrow \infty$ . It is interesting to note that although the sum of  $R_* \dot{\tau}_v$  and  $R_* \dot{\tau}_t$  is unity throughout the channel (or pipe), both transport terms change rapidly near the wall, achieving peak values of  $O(R_*)$ . Figure 4 shows the balance of the momentum transport terms at a low Reynolds number ( $R_* = 180$ ) for a turbu-

lent channel flow. Near the wall the transport terms are each large (up to 10 times the mean pressure gradient in magnitude) but of opposite sign. The net transport (of order unity) is thus the difference of two large terms (of order  $R_*$ ). Away from the wall both transport terms are of the same sign, having magnitudes of the order of the mean pressure gradient.

The main qualitative conclusion is that  $\tilde{y}$  depends on  $R_*$ . In the limit of large Reynolds numbers, it coincides with the peak location of the turbulence production (trivially), and with the location of the extrema of the mean momentum transport (both turbulent and viscous). The results indicate that there are slow Reynolds number changes, even very close to the wall, in the mean and fluctuating parts of the flow.

- <sup>1</sup>J. Laufer, The structure of turbulence in fully developed pipe flow, Technical Report No. NACA-1174, 1954.
- <sup>2</sup>P. S. Klebanoff, "Characteristics of turbulence in a boundary layer with zero pressure gradient," Technical Report No. NACA TR 1247, 1955.
- <sup>3</sup>K. R. Sreenivasan, The turbulent boundary layer, in *Frontiers in Experimental Fluid Mechanics*, edited by M. Gad-el-Hak (Springer-Verlag, Berlin, 1989), pp. 159–209.
- <sup>4</sup>S. J. Kline, W. C. Reynolds, F. A. Schraub, and H. M. Runstadler, "The structure of boundary layers," *J. Fluid Mech.* **30**, 741 (1967).
- <sup>5</sup>H. Eckelmann, "The structure of the viscous sublayer and the adjacent wall region in a turbulent channel flow," *J. Fluid Mech.* **65**, 439 (1974).
- <sup>6</sup>J. Laufer, "Investigation of turbulent flow in a two-dimensional channel," Technical Report No. NACA-1053, 1950.
- <sup>7</sup>J. Kim, P. Moin, and R. Moser, "Turbulence statistics in fully developed channel flow at low Reynolds number," *J. Fluid Mech.* **177**, 133 (1987).
- <sup>8</sup>G. Comte-Bellot, "Contribution a l'étude de la turbulence de conduite," Ph.D. thesis, University of Grenoble, 1963, Trans. P. Bradshaw, 1969 Turbulent flow between two parallel walls, ARC31609, FM 4102.
- <sup>9</sup>M. V. Zagarola, "Mean flow scaling of turbulent pipe flow," Ph.D. thesis, Department of Mechanical and Aerospace Engineering, Princeton University, 1996.